

# Hydraulic traits of deciduous tree species: Do lessons learned from arid climates translate to eastern US temperate forests?

Michael Benson<sup>1</sup>, Chelcy Miniati<sup>2</sup>, Andrew Oishi<sup>3</sup>, Sander Denham<sup>1</sup>, Jean-Christophe Domec<sup>4</sup>, Daniel Johnson<sup>5</sup>, Justine Missik<sup>6</sup>, Richard Phillips<sup>7</sup>, Jeffrey Wood<sup>8</sup>, and Kimberly Novick<sup>7</sup>

<sup>1</sup>Indiana University System

<sup>2</sup>USDA Forest Service, Southern Research Station, Coweeta Hydrologic Laboratory.

<sup>3</sup>USDA Forest Service, Southern Research Station, Coweeta Hydrologic Laboratory

<sup>4</sup>Bordeaux Sciences Agro

<sup>5</sup>University of Georgia

<sup>6</sup>Washington State University

<sup>7</sup>Indiana University

<sup>8</sup>University of Missouri

October 28, 2020

## Abstract

The coordination of plant leaf water potential ( $\Psi_L$ ) regulation and xylem vulnerability to embolism is fundamental for understanding the tradeoffs between carbon uptake and risk of hydraulic damage. A legacy of observations in drylands suggests plants with vulnerable xylem more carefully regulate  $\Psi_L$  than plants with resistant xylem. We synthesized over 1600  $\Psi_L$  observations, 122 xylem embolism curves, and xylem anatomical measurements of *Quercus alba* L., *Liriodendron tulipifera* L., and *Acer saccharum* Marsh. across ten contrasting forests to evaluate if the paradigm linking conservative  $\Psi_L$  regulation to vulnerable xylem applies to temperate deciduous trees. Additionally, we explored generalizable patterns of hydraulic trait acclimation in relation to forest age and climate. Contrary to the dryland paradigm, we found that the tree species with the most vulnerable xylem (e.g., *Q. alba*) regulated  $\Psi_L$  less strictly (anisohydric behavior) than the species with xylem more resistant to embolism (e.g., *A. saccharum* and *L. tulipifera*). This relationship was found across all sites, suggesting coordination among traits was largely unaffected spatio-temporal factors. Our findings indicate drought-response traits of temperate deciduous forest species are coordinated in fundamentally different ways than vegetation in arid climates.

## 1. Title Page

**Hydraulic traits of deciduous tree species: Do lessons learned from arid climates translate to eastern US temperate forests?**

Running Head: Hydraulic vulnerability in temperate US forests

Michael C. Benson<sup>1</sup>, Chelcy F. Miniati<sup>2</sup>, A. Christopher Oishi<sup>2</sup>, Sander O. Denham<sup>1</sup>, Jean-Christophe Domec<sup>3,4</sup>, Daniel M. Johnson<sup>5</sup>, Justine E. Missik<sup>6</sup>, Richard P. Phillips<sup>7</sup>, Jeffrey D. Wood<sup>8</sup>, Kimberly A. Novick<sup>1</sup>

<sup>1</sup> O'Neill School of Public and Environmental Affairs, Indiana University Bloomington. 1315 East Tenth Street, Bloomington, Indiana, 47405, USA

<sup>2</sup>USDA Forest Service, Southern Research Station, Coweeta Hydrologic Laboratory. 3160 Coweeta Lab Rd, Otto, North Carolina 28763 USA

<sup>3</sup>Bordeaux Sciences Agro, INRA UMR 1391 ISPA, Gradignan F – 33170, France

<sup>4</sup>Nichols School of the Environment, Duke University, Durham, North Carolina 27708

<sup>5</sup>Warnell School of Forestry and Natural Resources, University of Georgia, Athens, GA 30602, USA

<sup>6</sup>Laboratory for Atmospheric Research, Department of Civil and Environmental Engineering, Washington State University, Pullman, WA, USA

<sup>7</sup>Department of Biology, Indiana University – Bloomington. 1001 E 3rd St, Bloomington, Indiana 47405, USA

<sup>8</sup>School of Natural Resources, University of Missouri – Columbia. 1111 Rollins St., Columbia, Missouri, 65211, USA

Author for correspondence:

*Michael C. Benson*

*Tel: +1 (405) 443 7070*

*Email: micbenso@iu.edu*

### 3. Keyword Index

*Acer saccharum* Marsh., embolism vulnerability, isohydricity, leaf water potential, *Liriodendron tulipifera* L., temperate deciduous forests, *Quercus alba* L.

### 4. Introduction

When plants are water-limited, adaptive stomatal closure can alleviate stress on the plant hydraulic system by reducing water loss to the atmosphere and preventing the development of excessively low water potentials within the plant (Buckley, 2005). However, because stomatal closure down-regulates both water and carbon fluxes at the leaf surface, there can be deleterious consequences for plant health from reduced photosynthesis. Tree species differ widely in their ability to regulate plant water status. Often, this behavior is described along an isohydric spectrum by characterizing plant regulation of leaf water potential ( $\Psi_L$ ) as soil water potential ( $\Psi_S$ ) declines (e.g.,  $\partial\Psi_L/\partial\Psi_S$ ) (Tardieu & Simonneau, 1998; McDowell *et al.* , 2008; Klein, 2014; Matheny *et al.*, 2016; Meinzer *et al.* , 2016). More anisohydric species loosely regulate stomatal conductance with rising evaporative demand, allowing  $\Psi_L$  to decline as soils dry (Martínez-Vilalta *et al.* , 2014). In contrast, more isohydric species strictly regulate plant water loss by closing their stomata to minimize  $\Psi_L$  decline. A less negative  $\Psi_L$  maintains the turgor pressure necessary for leaf cell growth and expansion and is an important factor determining the risk of damage to the hydraulic system from xylem embolism (Tyree & Zimmermann, 2013).

Embolism occurs when hydrologic stress causes excessively large tension forces (e.g., very low water potential) in the plant hydraulic system. As a result, xylem conduits become cavitated and embolized, and no longer function to transport water (Tyree & Sperry, 1989; Davis *et al.* , 1999). The coordination of  $\Psi_L$  regulation and vulnerability of xylem tissues is therefore fundamental for understanding the tradeoffs between carbon uptake and risk of hydraulic damage across vegetative species. The prevailing paradigm is that trees with more vulnerable xylem tend to be more isohydric (Bond & Kavanagh, 1999; Shultz, 2003; McDowell *et al.* , 2008; Taneda & Sperry, 2008; Choat *et al.* , 2012; Plaut *et al.* , 2012; Meinzer *et al.* , 2014; Skelton *et al.*, 2015; Sperry & Love, 2015; Garcia-Forner *et al.* , 2016), as they operate with smaller safety margins to xylem embolism and therefore require careful regulation of  $\Psi_L$  to avoid hydraulic damage.

This view on the coordination of stomatal regulation of  $\Psi_L$  and xylem vulnerability is implicit in the recent incorporation of new plant hydraulic schemes into terrestrial ecosystem models (TEM) (Naudts *et al.* , 2015;

Kennedy *et al.*, 2019; Mirfenderesgi *et al.*, 2019). The TEM frameworks differ in the way that hydraulics and leaf-level gas exchange processes are mathematically linked; however, all fundamentally relate the stomatal sensitivity to declining plant or soil water potential to the shape of the xylem vulnerability curve. The ability of a model to link xylem vulnerability to isohydric behavior is even viewed as an important check on a model’s functionality (Sperry & Love, 2015).

Much of what we know about coordination between  $\Psi_L$  and xylem vulnerability to embolism has relied on a legacy of observations from dryland ecosystems (McDowell *et al.*, 2008; Taneda & Sperry, 2008; Plaut *et al.*, 2012; Skelton *et al.*, 2015), where plants are generally adapted to arid environments, but excessive drought conditions have promoted widespread mortality (Macalady & Bugmann, 2014; Meddens *et al.*, 2015). Less is known about the coordination of these hydraulic traits in more temperate forests, where drought stress is often less severe than dryland ecosystems but is predicted to increase in frequency and severity into the future (Dai, 2011; Novick *et al.*, 2016). Eastern US temperate forests are characterized by tall canopies and dense foliage cover in which plants must compete for space (Olivier *et al.*, 2016). While drought-induced mortality periodically occurs in these ecosystems (Elliott & Swank, 1994; Dietze & Moorecraft, 2011; Wood *et al.*, 2018), trees must balance conserving hydraulic function with maintaining sufficient productivity and growth to compete for light. Given these constraints, it is not clear that water-use strategies which adhere to strict coordination between stomatal regulation and xylem vulnerability should necessarily confer a universal advantage across diverse ecosystems.

Our understanding of tradeoffs between xylem vulnerability and  $\Psi_L$  regulation is further challenged by a tenuous understanding of intraspecific patterns of vulnerability (Anderegg, 2015). Species which encompass broad climate envelopes sometimes acclimate their xylem tissues to thrive across diverse environmental conditions (Maherali & Delucia, 2000; Herbette *et al.*, 2010; Wortemann *et al.*, 2011). Coordination of hydraulic traits may also change over time, reflecting long-term, plastic responses to drought such as changes in xylem anatomy (e.g., vessel diameter) that produce more resistant xylem (Maherali *et al.*, 2006). Understanding intraspecific embolism vulnerability in both space and time is particularly important for eastern US deciduous forests, which are species-rich, environmentally diverse, and characterized by uneven-aged stands from a legacy of management and disturbance (Pan *et al.*, 2011). Nevertheless, spatio-temporal patterns of hydraulic vulnerability across this region are poorly understood.

In this paper, we focus on identifying inter- and intraspecific patterns of hydraulic traits in eastern US deciduous forests that determine plant responses to both vapor pressure deficit ( $D$ ) and declining soil moisture, both of which affect the evolution of  $\Psi_L$  and stomatal regulation thereof (Tardieu & Simonneau 1998; Domec & Johnson, 2012; Novick *et al.*, 2019). Our analysis also explicitly tests assumptions that guide the parameterization of plant hydraulics in TEMs. Our work is guided by the overarching question: Do the drought response paradigms developed from observations of dryland vegetation apply in temperate deciduous forests of the eastern US? To answer this question, we tested the following three hypotheses:

- 1) Trees invest in more resistant xylem when growing in regions that more regularly experience moisture stress.
- 2) Stem tissues are more vulnerable to embolism in shorter, younger stands than in taller, more mature stands, because taller trees will have developed more resistant xylem to overcome additional constraints on water movement from increased canopy height (McDowell *et al.*, 2002; Novick *et al.*, 2009).
- 3) Stem tissues from trees that display anisohydric behavior will be more resistant to hydraulic dysfunction than trees that more rapidly close their stomata to limit  $\Psi_L$  decline (e.g., isohydric behavior). This hypothesis reflects the prevailing paradigm, based largely on dryland studies, that the vulnerability of xylem tissues to embolism is linked to more isohydric behavior.

To test these hypotheses, we analyzed stem xylem anatomy, stem embolism vulnerability, and  $\Psi_L$  observations of three common deciduous forest species with contrasting xylem anatomy and stomatal regulation, *Acer saccharum* Marsh., *Quercus alba* L., and *Liriodendron tulipifera* L. We conducted this study across ten forest stands of differing age and climates that broadly represented moisture availability for deciduous

vegetation across the eastern US. We characterized the plasticity of critical hydraulic traits that determine drought-tolerance and productivity. Additionally, we sought to understand if the functional coordination of  $\Psi_L$  regulation and risk of xylem dysfunction commonly observed in dryland vegetation is indicative of drought-response behavior of temperate forests.

## 5. Materials and Methods

### 5.1 Study sites

We selected ten forest stands across four regions in the eastern US that spanned a hydroclimatological gradient (Fig. 1). Four of the stands were ~85-year-old temperate deciduous forest AmeriFlux network sites (US-MMS, US-CWT, US-Dk2, and US-MOz) in the states of Indiana (IN), North Carolina (NC), and Missouri (MO). The gradient approach allowed us to understand how key plant hydraulic traits varied as a function of climate. Additionally, The ~85-year-old stands in IN and NC were each end-members of a chronosequence (including ~15- and ~35-year-old stands co-located within 20 km of the ~85-year-old stand). The chronosequences in NC and IN allowed us to investigate how the relationship between  $\Psi_L$  regulation and vulnerability to hydraulic failure varied with stand age in regions experiencing a similar climate.

#### *Indiana chronosequence stands:*

The ~85-year-old (IN 85yo) (39° 19' 23.52", -86° 24' 47.16") and ~35-year-old (IN 35yo) (39° 19' 19.87", -86° 28' 51.92") IN stands were located in Morgan-Monroe State Forest, a temperate forest with 1032 mm mean annual precipitation and 10.85 °C mean annual temperature (Roman *et al.*, 2015). Dominant species were *A. saccharum*, *L. tulipifera*, *Q. alba*, *Sassafras albidum* Nutt., *Quercus rubra* L., and dense *Lindera benzoin* L. understory. Mean canopy height was 20 m and 30 m in IN 35yo and IN 85yo, respectively. Deep silt clay loam soils characterized the sites (90–120 cm). The ~15-year-old stand (IN 15yo) (39° 13' 10.93", -86° 32' 30.96") was a nearby (<20 km) regenerating planting with similar species composition located at The Indiana University Research and Teaching Preserve's Bayles Road site. There, 5-year-old saplings of common Indiana forest tree species were planted in 2006 at a spacing of 5.25m × 5.25m and in random 12 × 12 arrangements (Flory & Clay, 2010). Mean canopy height in IN 15yo was 5 m.

#### *Western North Carolina chronosequence stands:*

The ~85-year-old (NC\_W 85yo) (35° 3' 33.12", -83° 25' 39") and ~35-year-old (NC\_W 35yo) (35° 3' 55.22", -83° 26' 17.54") stands in the western NC chronosequence were located in the Coweeta Basin, at the USDA Forest Service Coweeta Hydrologic Laboratory. The site is characterized as a mesic forest with 1800 mm of mean annual precipitation and 13 °C mean annual temperature (Oishi *et al.*, 2018). Mean canopy height was 17 m and 35 m in NC\_W 35yo and NC\_W 85yo, respectively. Soils were fine-loamy with a variable depth of approximately 35 to >90 cm. The NC\_W 85yo was a mature, secondary forest dominated by *L. tulipifera*, *Q. alba*, *Acer rubrum* L., *Betula lenta* L., and dense *Rhododendron maximum* L. understory. The NC\_W 35yo stand had similar species composition, but was clearcut in 1976-1977 (Swank & Webster, 2014). The ~15-year-old NC stand (NC 15yo) (35° 10' 47.71", -83° 29' 44.98") was a selectively harvested stand located nearby (<20 km) in the Nantahala National Forest with similar species composition. Mean canopy height in NC\_W 15yo was 4.5 m.

#### *Eastern North Carolina chronosequence stands:*

The ~85-year-old (NC\_E 85yo), ~35-year-old (NC\_E 35yo), and ~15-year old (NC\_E 15yo) eastern NC chronosequence stands were located in the Blackwood Division of Duke Forest (35° 58' 24.89", -79° 6' 1.55"). Mean annual precipitation (1945–2015) for the area is 1144 ± 162 mm, with 619 ± 116 mm falling between April and September. Annual mean temperature is 14.36 °C. NC\_E 85yo was a naturally established stand comprised of mixed hardwood species *Q. alba*, *Quercus michauxii* Nutt., *L. tulipifera*, *Liquidambar styraciflua* L., and hickory species *Carya tomentosa* Sarg. and *Carya glabra* Miller with a mean canopy height of 27.5 m (Oishi *et al.*, 2010). NC\_E 35yo was located less than 4 km from NC\_E 85yo and was part of the former Duke FACE project ambient plots. This site was clear-cut in 1982 to remove a 50-year-old mixed pine forest and was replanted in 1983. The stand was dominated by *Pinus taeda* L. but *Q. alba*, *L. tulipifera*,

*Acer rubrum* L., *L. styraciflua*, *Cornus florida* L. and *Prunus serotina* occurred in the understory and stand gaps. Mean height of the mid-canopy *Q. alba* and *L. tulipifera* trees in the NC\_E 35yo stand was 15.1 m. Soils were gravelly loam of the Iredell series with majority of the rooting zone occurring at 45–65 cm depth (Domec *et al.*, 2012).

*A. saccharum* trees were sampled in the NC\_E chronosequence from an additional lowland hardwood stand located 15 km from the ones described above. *Fagus grandifolia* Ehrh. was the dominant canopy tree species of this lowland hardwood site, but *Q. alba*, *Q. rubra*, *L. styraciflua*, and *A. saccharum* occurred frequently in the understory. This site was also part of the Duke Forest but was characterized by a deep and well-drained soil with minimal disturbance. The mean height of ~15 and ~35 years old *A. saccharum* trees were 9.2 and 19.5 m, respectively.

#### Missouri stand:

The ~85-year-old MO stand (MO 85yo) (38° 44' 38.76", -92° 12' 0") was located in the University of Missouri's Baskett Wildlife Research and Education Area. It is a comparatively xeric secondary oak-hickory forest, where mean annual temperature is 12.11 °C and mean annual precipitation is 986 mm. While this site received similar annual precipitation to IN and NC\_E, high precipitation variability and comparatively shallow silt loam soils imposed frequent and severe physiological drought (Gu *et al.*, 2015; Gu *et al.*, 2016). Dominant species were *A. saccharum*, *Q. alba*, *Quercus velutina* Lam., *Carya ovata* (Mill.) K. Koch, and *Juniperus virginiana* L. Mean canopy height was 18.5 m.

## 5.2 Study Species

Tree species were selected to focus on a parsimonious set of species such that within each region, we studied at least one relatively isohydric species and at least one relatively anisohydric species (using results from previous work, including Roman *et al.*, 2015 and Vose & Elliot, 2016). Overall, we targeted *A. saccharum* (isohydric), *L. tulipifera* (isohydric), and *Q. alba* (anisohydric) and sampled each of these species when present. In MO 85yo we sampled *A. saccharum* and *Q. alba*. In the NC\_W chronosequence we sampled *L. tulipifera* and *Q. alba* at each respective stand. In the NC\_E chronosequence we sampled *Q. alba* and *L. tulipifera* in the 85yo and 35yo stands, and *A. saccharum* in the neighboring lowland hardwood stand. In the IN 15yo and IN 35yo, we sampled *L. tulipifera* and *Q. alba*. In IN 85yo we sampled *Q. alba*, *A. saccharum*, and *L. tulipifera*. Tree species and climate conditions across stands and regions are summarized in Table 1.

## 5.3 Characterizing midday $\Psi_L$ regulation

Periodic midday  $\Psi_L$  measurements (10:00–16:00 local time) were compiled from a dataset of over 1600 observations collected throughout the growing seasons of 2011–2017. On each measurement day, one to five samples were collected from one to three trees per species from the upper third of the canopy. After excision,  $\Psi_L$  was measured using a pressure chamber (PMS Instruments, Corvallis, OR, USA) (Turner, 1988) immediately in the field, or after being transferred back to the lab in a humidified bag stored in a chest cooler. All together, we made 704, 178, and 757  $\Psi_L$  observations of *L. tulipifera*, *A. saccharum*, and *Q. alba*, respectively. The number of  $\Psi_L$  observations and sampling days varied across the stands, but  $\Psi_L$  was measured on 4–51 different days at each specific stand. Moreover, these days were distributed across the growing season, including sampling at the beginning (June) and end (September) to permit observation throughout dynamic seasonal changes of moisture conditions.

While drought response behavior is commonly described along an isohydric spectrum (e.g.,  $\partial\Psi_L/\partial\Psi_S$ ), often a species' relative degree of isohydricity is inconsistent from one stand to the next (Martínez-Vilatla & Garcia-Forner, 2017). For example, Roman *et al.* (2015) reported  $\partial\Psi_L/\partial\Psi_S$  for *Quercus* spp. in southern Indiana was 1.31 during a severe regional drought. Bahari *et al.* (1985) observed that  $\partial\Psi_L/\partial\Psi_S$  was 0.28 for *Q. alba* in the Missouri Ozarks, while a decade later, Loewenstein & Pallardy (1998) observed that  $\partial\Psi_L/\partial\Psi_S$  was 0.61 for *Q. alba* in the same region. These inconsistent results likely reflect the fact that the degree of isohydricity, defined as  $\partial\Psi_L/\partial\Psi_S$ , is complicated by environmental interactions (Hochberg *et al.*, 2018), including site-to-site variations in  $D$  (Novick *et al.*, 2019), or when the magnitude of soil water deficit during

the sampling period is insufficient to capture stress responses (Martínez-Vilatla & Garcia-Forner, 2017). This is particularly challenging in mesic ecosystems with frequently saturated soils (e.g., NC\_W chronosequence stands), where the seasonal variation of midday  $\Psi_L$  patterns may be driven by stomatal sensitivity to  $D$  rather than declines in soil moisture (Novick *et al.*, 2019). To overcome these challenges for this study, the degree of isohydricity was characterized by quantifying seasonal midday  $\Psi_L$  variability with the assumption that more anisohydric trees, which more readily allow  $\Psi_L$  to drop in response to soil moisture decline and/or increasing  $D$ , will have a greater seasonal range of  $\Psi_L$  than more isohydric trees. To minimize error associated with uncharacteristic behavior during spring leaf out and fall senescence,  $\Psi_L$  data used for this analysis were constrained to a period of relatively stationary leaf area index (days of year 150–270).

#### 5.4 Xylem embolism vulnerability curves

Vulnerability to hydraulic failure was estimated with cavitation-induced embolism curves. The relationship between the loss of stem hydraulic function and xylem water potential ( $\Psi_x$ ) (MPa) was measured on stem tissues ( $n = 3-5$ ) from 2–3 trees per species at each stand, resulting in 6–12 curves per species per stand, or 165 total curves. Vulnerability curves were generated using the air-injection technique (Sperry & Saliendra, 1994; Johnson *et al.*, 2016). Branches were harvested from the upper third of the canopy, and stem samples ~20 cm in length were collected from the terminal bud of felled branches. Samples were stored at 5 °C submerged in deionized water that was replenished daily and were measured within two weeks of collection.

We used a pressure flow meter (XYLEM embolism meter, Bronkhorst, Montigny les Cormeilles, France) to measure stem hydraulic conductivity ( $K_{stem}$ ) ( $\text{kg m}^{-1}\text{s}^{-1} \text{MPa}^{-1}$ ), and a pressure sleeve (Scholander Pressure Chamber model 1505D, PMS Instruments, Corvallis, OR, USA) to facilitate air-injection. Samples were rehydrated by flushing native embolism in submerged deionized water under vacuum for 24+ hours. Following rehydration, stem samples were exposed to positive air pressure in 0.5 to 1.0 MPa increments until >85% reduction of maximum  $K_{stem}$  ( $K_{max}$ ) ( $\text{kg m}^{-1}\text{s}^{-1} \text{MPa}^{-1}$ ) was reached or the applied pressure approached instrument limitation. We then corrected  $K_{stem}$  to 20 °C to account for changing viscosity of water with temperature ( $K_{20}$ ) ( $\text{kg m}^{-1} \text{s}^{-1} \text{MPa}^{-1}$ ). The percent loss of conductivity (PLC) (%) at a given applied pressure was calculated as:

$$PLC = 100 \times \left(1 - \frac{K_{20}}{K_{max}}\right) \quad (1)$$

The relationship between PLC and  $\Psi_x$  was then fitted to the sigmoid function provided by Maherli *et al.*, (2006):

$$PLC = \frac{100}{[1 + \exp(\alpha(\Psi_x - b))]} \quad (2)$$

where  $a$  and  $b$  are empirical coefficients determined using nonlinear curve fitting (MATLAB, The Mathworks Inc., Natick, MA, USA; v. R2018a). The fitted relationship was then used to calculate the  $\Psi_x$  at which 12% PLC (P12) (MPa) and 50% PLC (denoted as  $b = P50$ ) (MPa) occurred. The pressures at 12% PLC ( $P12 = 2/a + b$ ) were determined as described by Domec & Gartner (2001). The value P12, termed the air entry point, is an estimate of the xylem tension at which the resistance to air entry of pit membranes within the conducting xylem is overcome and cavitation and embolism begin.

While the air-injection method is commonly used to assess vulnerability to embolism (Sperry & Saliendra, 1994; Johnson *et al.*, 2016), measurement artifacts from destructive sampling, such as the presence of open vessels, may over-estimate *in-situ* vulnerability (Martin-StPaul *et al.*, 2014). This bias may be particularly important for species like *Q. alba*, which has long xylem vessels that can reach up to several meters in length (Cochard & Tyree, 1990). We therefore took multiple steps to minimize bias from open vessel artifacts. First, we sampled young distal tissues from branch apices, which have relatively short vessels (Cochard & Tyree, 1990). Second, before curve generation, the presence of open vessels was checked using a modified infiltration technique following Cochard *et al.* (2010), and samples with suspected open vessels were subsequently not used for embolism curve measurements.

As a third step, we considered the shape of the vulnerability curve. It has been suggested that embolism curves that are conspicuously “r” shaped are likely affected by open vessel artifacts, and that “s” shaped

curves more accurately represent *in-situ* vulnerability (Torres-Ruiz *et al.* , 2014; Skelton *et al.*, 2018). We defined an “s” shape curve as one that lost less than 7.5% of its  $K_{max}$  as  $\Psi_x$  declined from 0 to -0.5 MPa and screened our dataset to use only these curves for the subsequent analyses. We performed the analysis at alternative cutoff thresholds of 3%, 5%, and 10% loss of  $K_{max}$  , but there were no noticeable effect on the results. Comparing the “s” shaped data to the “r” shaped data for *Q. alba* and *L. tulipifera* showed that “r” shaped curves tended to have statistically higher P12 and P50 than “s” shaped curves (Fig. 2). No *A. saccharum* sample displayed “r” shape curves by our criteria. For species with more vulnerable xylem tissues (e.g., *Q. alba* ), including both “s” and “r” shaped curves did not markedly change the estimated P50 (Fig. 2f). Nevertheless, “r” shaped curves for any species were not included for subsequent analyses, resulting in a total of 40, 56, 26 suitable “s” shaped curves for *L. tulipifera* , *Q. alba* , and *A. saccharum* , respectively (or ~74% of the original 165 curves).

### 5.5 Xylem anatomy

To understand how changes in xylem vulnerability are linked to variations in xylem anatomy, we measured vessel lumen area and vessel density on transverse sections (~40  $\mu\text{m}$  diameter) extracted from stems of *Q. alba* and *L. tulipifera* from the NC.W, IN, and NC.E chronosequence stands that were used for embolism vulnerability measurements. Stem samples were softened by boiling in deionized water (Schweingruber, 2007) and sectioned by hand using a fresh razor blade. Before analysis under the microscope, the transverse sections were dried in an oven at 150 °C. Slides from the NC.W and IN chronosequences were imaged with a stereoscope and color camera at 150 $\times$  magnification (Leica M205F, Leica DFC310FX, Leica Microsystems, Heerbrugge, Switzerland). Vessel lumen area and density were then calculated using threshold balance manipulation and the analyze particle function of ImageJ v1.6 software (National Institutes of Health, USA) (Scholz *et al.* , 2013). Slides from the NC.E chronosequence were photographed at 100 $\times$  and 200 $\times$  magnifications and analyzed using the Motic Images Advanced 3.2 software (Motic Corporation, Zhejiang, China).

### 5.6 Data processing and analysis

We investigated differences in P12 and P50 across species and stands (hypotheses 1 and 2) with a two-way ANOVA, where species and stand age were fixed factors and region was a blocking factor. We compared vessel density and lumen area between *Q. alba* and *L. tulipifera* stems with a two-way ANOVA, where species and stand age were fixed factors. We removed region as a blocking factor because there was no significant region or region interaction effect at  $p = 0.05$ . The relationships between xylem anatomy (e.g., vessel density and vessel lumen area) and embolism thresholds (e.g., P12 and P50) were assessed with linear regression within and across species.

We analyzed the relationship between embolism thresholds and isohydricity (hypothesis 3) in two ways. First, we compared embolism thresholds between isohydric and anisohydric species using a two-tailed *t*-test. Second, we investigated this relationship in the context of a hydraulic safety margin ( $\Psi_{\text{safety}}$ ) (MPa). Safety margins to P12 ( $\Psi_{\text{safety, P12}}$ ) (MPa) and P50 ( $\Psi_{\text{safety, P50}}$ ) (MPa) were calculated using the following equation (Domec & Gartner, 2001; Delzon & Cochard, 2014):

$$\Psi_{\text{safety}} = \Psi_{L,\text{min}} - \Psi_{\text{thresh}} \quad (3)$$

where  $\Psi_{L,\text{min}}$  (MPa) is the minimum  $\Psi_L$  of a given species in a specific stand, and  $\Psi_{\text{thresh}}$ , (MPa) is mean embolism threshold (e.g., P12 or P50) for the same species in the same stand. A negative  $\Psi_{\text{safety}}$  suggests a high level of xylem embolism, while a positive  $\Psi_{\text{safety}}$  suggests a window of safety from critical levels of xylem dysfunction (Johnson *et al.* , 2016). We then performed a linear regression between  $\Psi_{\text{safety}}$  and  $\Psi_L$  interquartile range across species and stands.

All ANOVA analyses were performed at the  $\alpha = 0.05$  level and were followed by a Tukey post-hoc test for significant main effects. Significant interaction terms were assessed by pairwise comparison of least square means.

## 6. Results

## 6.1 Spatio-temporal variation in embolism vulnerability

We found little variation in embolism vulnerability across stands, though clear species differences were observed. Across all stands, mean embolism thresholds were markedly different across species ( $F_{ndf,ddf} = 149.87, p = 0.001$  for P12, and  $F_{ndf,ddf} = 169.62, p = 0.003$  for P50, Fig. 3). At the P50 threshold however, we detected some variability arising from the interaction between species and age ( $F_{ndf,ddf} = 18.88, p = 0.017$ , Table 2) and age and region ( $F_{ndf,ddf} = 21.312, p = 0.016$ , Table 2). Specifically, we found that *A. saccharum* P50 differed between young (15yo) and intermediate (35yo) stands, although embolism vulnerabilities were invariant across stand ages for *Q. alba* and *L. tulipifera* (Fig 4a). Additionally, across all species, young stands (15yo) had more vulnerable xylem in the mesic NC\_W chronosequence stands than in the drier IN and NC\_E stands; however, this pattern was not observed for the 35yo and 85yo age classes (Fig 4b). In general, *Q. alba* had the most vulnerable xylem while *A. saccharum* had the least (Fig. 3). Mean P12 across all stands were -1.09 MPa (SE = 0.06), -1.65 MPa (SE = 0.10), and -2.75 MPa (SE = 0.20) and mean P50 was -2.72 MPa (SE = 0.09), -3.91 MPa (SE = 0.12), and -4.77 MPa (SE = 0.18) for *Q. alba*, *L. tulipifera*, and *A. saccharum*, respectively.

## 6.2 Relationship between xylem anatomy and embolism vulnerability

Xylem anatomy varied considerably between diffuse-porous *L. tulipifera* and ring-porous *Q. alba*. Tissues of *L. tulipifera* consistently had smaller mean vessel lumen area ( $F_{ndf,ddf} = 169.953, p = <0.001$ , Fig. 5) and larger mean vessel densities ( $F_{ndf,ddf} = 270.636, p = <0.001$ , Fig. 6) than *Q. alba*. Mean vessel lumen area was not influenced by local climate or age (region, age, or interactions NS, Table 3).

Xylem anatomy had moderate explanatory power for tissue-level embolism vulnerability. Across species, stems with larger vessel lumen area (Fig. 5d) and lower vessel densities (Fig. 6d) approached 50% loss of hydraulic function at lower  $\Psi_x$  ( $R^2 = 0.335, p = <0.001$  for lumen area, and  $R^2 = 0.268, p = <0.001$  for vessel density). Patterns with P12 were similar, but generally weaker than in relation to P50. Specifically, tissues with larger mean vessel lumen area tended to approach 12% loss of hydraulic function at lower  $\Psi_x$  relative to tissues with smaller mean lumen area ( $R^2 = 0.112, p = 0.005$ , Fig. 5b). Tissues with greater vessel densities were generally more embolism-resistant at P12 ( $R^2 = 0.08, p = 0.019$ , Fig. 5b). However, this pattern was contradicted by *Q. alba*, where stems with greater vessel densities were more vulnerable to 12% loss of hydraulic function ( $R^2 = 0.256, p = 0.002$ , Fig. 6b).

## 6.3 Diagnosing leaf water status and leaf hydraulic strategy

Seasonal midday  $\Psi_L$  values were variable across species and stands, but in general, *Q. alba* experienced a lower overall midday  $\Psi_L$  and a broader range. Larger species-specific declines in midday  $\Psi_L$  occurred in the more arid forest stands (e.g., NC\_E chronosequence and MO), while the smallest occurred in NC 15yo (Fig. 7a). Leaf hydraulic strategy was primarily determined by species ( $F_{ndf,ddf} = 22.20, p = <0.001$ ), and no influence of age on mean  $\Psi_L$  interquartile ranges were detected (age and age-species interactions NS). The *L. tulipifera* and *A. saccharum* mean  $\Psi_L$  interquartile ranges were indistinguishable, but significantly lower than *Q. alba* (Fig. 7b); mean  $\Psi_L$  interquartile ranges across stands were 0.709 MPa (SE = 0.040), 0.358 MPa (SE = 0.022), and 0.372 MPa (SE = 0.098) for *Q. alba*, *L. tulipifera*, and *A. saccharum*, respectively. Overall, *Q. alba* displayed more anisohydric behavior while *L. tulipifera* and *A. saccharum* were more isohydric.

## 6.4 Ρελατιονσηπ βετωεεν $\Psi_L$ ρεγυλατιον ανδ υλνεραβιλιτιψ το ηψδραυλις φαιλυρε

The most anisohydric species (*Q. alba*) in our study possessed xylem that was more vulnerable to embolism than the more isohydric species. This pattern was consistent at both P12 and P50, where *Q. alba* mean embolism thresholds were significantly greater ( $p = <0.001$  for P12 and P50, respectively) than the more isohydric *L. tulipifera* and *A. saccharum* (Fig 8). Mean  $\Psi_{safety,P12}$  values were -1.77 MPa (SE = 0.166), -0.35 MPa (SE = 0.078), and 0.63 MPa (SE = 0.319), and mean  $\Psi_{safety,P50}$  values were -0.147 MPa (SE = 0.196), 1.94 MPa (SE = 0.143), and 2.634 MPa (SE = 0.351) for *Q. alba*, *L. tulipifera*, and *A. saccharum*, respectively. Moreover, the degree of isohydricity (as defined by seasonal  $\Psi_L$  interquartile range) was strongly associated with risk of xylem dysfunction such that ~60% of the variability in  $\Psi_{safety}$  across stands

was explained by a tree’s relative  $\Psi_L$  control (Fig. 9).

Across all stands,  $\Psi_{\text{safety}}$  values were smallest and often negative for *Q. alba*, suggesting that *Q. alba* operated at lower proportional level of its maximum hydraulic function relative to *L. tulipifera* and *A. saccharum*. Likewise, estimated *in-situ*  $K_{\text{stem}}$  values were consistently lower for *Q. alba* than other co-occurring study species. For example, in the NC\_E chronosequence, where  $\Psi_{\text{safety}}$  were often smallest, estimated *in-situ*  $K_{\text{stem}}$  was  $0.30 \text{ kg m}^{-1} \text{ s}^{-1} \text{ MPa}^{-1}$  (SE = 0.133) for *Q. alba*, accounting for a 67.1% reduction of  $K_{\text{max}}$ . By comparison, estimated *in-situ*  $K_{\text{stem}}$  for *L. tulipifera* and *A. saccharum* in these sites were  $1.12 \text{ kg m}^{-1} \text{ s}^{-1} \text{ MPa}^{-1}$  (SE = 0.148) and  $0.62 \text{ kg m}^{-1} \text{ s}^{-1} \text{ MPa}^{-1}$  (SE = 0.04) (accounting for a 18.79% and 7.02% reduction of  $K_{\text{max}}$ , respectively).

## 7. Discussion

We tested three hypotheses to assess variability and coordination of key plant hydraulic traits across ten deciduous forest stands. We found little support for hypotheses 1 and 2; we observed that variation of embolism vulnerability was better explained by species than intraspecific factors. While we detected some region and age effects, variation in vulnerability was principally determined by the large species effect. Additionally, our results did not confirm hypothesis 3, which predicted stricter  $\Psi_L$  regulation would be associated more vulnerable xylem. Contrary to the prevailing paradigm, we found that anisohydric *Q. alba* possessed stem tissues more vulnerable to embolism than isohydric *L. tulipifera* and *A. saccharum*. Moreover, we found that *Q. alba* had small or negative  $\Psi_{\text{safety}}$ , such that its anisohydric behavior likely occurred with a substantial hydraulic cost.

### 7.1 Why were embolism thresholds invariant with climate and stand age?

We found little variation in hydraulic vulnerability across climate and age. This result, however, must be reconciled with the body of work demonstrating vegetation’s capacity to acclimate xylem to pedo-climatic conditions (Awad *et al.*, 2010; Durante *et al.*, 2011; Gea-Izquierdo *et al.*, 2012). The clearest trends of acclimation are often found in manipulation experiments (Beikircher & Mayr, 2009; Awad *et al.*, 2010). However, surveys of hydraulic traits across species’ ranges have found these patterns more ambiguous (Martínez-Vilalta *et al.*, 2009; Wortemann *et al.*, 2011; Charra-Vaskou *et al.*, 2012; Lamy *et al.*, 2014).

The similarity across climate observed here may be evidence that acclimation reflects a broader set of morphological changes to the whole-plant hydraulic architecture, rather than simple adjustments to stem xylem traits (Lamy *et al.*, 2014). Modifications to other drought-tolerant traits may therefore explain how *Q. alba*, *L. tulipifera*, and *A. saccharum* establish dominance across diverse climate ranges. Such acclimation may include modifications to leaf:sapwood area ratio (Addington *et al.*, 2006; Martínez-Vilalta *et al.*, 2009), root:leaf area ratio (Sperry *et al.*, 2002), fine root turnover (Meier & Leuschner, 2008), or vulnerability of root tissues (Alder *et al.*, 1996; Wolfe *et al.*, 2016).

The absence of xylem acclimation with age/height may similarly reflect a reliance on morphological changes to alleviate emerging hydraulic constraints as forests mature. As canopies grow in height, greater xylem tension and pathlength resistance restricts hydraulic transport to canopy leaves (McDowell *et al.*, 2002; Novick *et al.*, 2009). To cope with these constraints, species representing the extremes of tree height often show strong patterns of increased stem embolism resistance with increased height in the canopy, indicative of acclimation (Burgess *et al.*, 2006; Ambrose *et al.*, 2009). Although age effects on embolism thresholds were minimal across stands, age also had little impact on  $\Psi_L$  decline. Thus, age-related constraints may have been mitigated through whole-plant adjustments that reduce damaging plant water potential gradients, rather than increased xylem resistance.

### 7.2 The perplexing case of *Q. alba*

Our finding that *Q. alba* had the most vulnerable xylem was unexpected. *Quercus* species are often considered more drought tolerant than many co-dominants, attributed to their morphological and physiological adaptations that allow them to withstand soil moisture deficits (Abrams, 2003). Our results complicate this perspective. We found that *Q. alba* had particularly high P50 (consistent with previous work: Maherali *et al.*

., 2006; Kannenberg *et al.*, 2020) but were also more anisohydric (consistent with previous work: Thomsen *et al.* ., 2013, Roman *et al.* ., 2015; Meinzer *et al.* ., 2017). Additionally, we found that  $\Psi_{\text{safety}}$  was often negative for *Q. alba* , suggesting these trees were remarkably vulnerable to drought.

The  $\Psi_{\text{safety}}$  is widely used to characterize risk of hydraulic dysfunction (Choat *et al.* ., 2012; Delzon & Cochard, 2014; Johnson *et al.* ., 2016); however, its use as a predictor for drought-susceptibility must be carefully evaluated. Drought-susceptibility is not explicitly determined by risk of xylem dysfunction, but in the context of a plant’s ability to cope with hydraulic damage (Meinzer & McCulloh, 2013). It is widely accepted that refilling of embolized conduits occurs in many species, especially ring-porous species (Brodersen *et al.* ., 2010; Ogasa *et al.* ., 2013; Trifilò *et al.* ., 2019; Zeppel *et al.* ., 2019). Refilling could therefore explain how *Q. alba* tolerates drought while possessing vulnerable xylem. Moreover, *Q. alba* bears only a few hydraulically active sapwood rings (<10), with the newest rings being the most efficient at moving water (Phillips *et al.* ., 1996). Therefore, even without any xylem refilling, *Q. alba* could potentially repair a 50% loss of conductivity in fewer than five years just by the production of new yearly rings.

It is also not clear that *Q. alba* rely on the entire depth of sapwood to actively conduct water (Cochard & Tyree, 1990). In a related study from IN 85yo, Yi *et al.* . (2017) found that *Q. alba*’s inner sapwood conducted a more significant fraction of water during drought, with water transport largely restricted to outer rings during well-watered periods. It is important to note that our methods, and specifically the rehydration of branches to flush native embolisms, permit an evaluation of the vulnerability of the entire sapwood depth (not the portion thereof actively involved in water transport). Finally, internal water storage can also play an important role in determining the relationship between leaf gas exchange and stem xylem traits. Ring-porous species are known to use smaller amounts of stored water than diffuse-porous species because of their low number of active rings (Köcher *et al.* ., 2013). Additionally, *Q. alba* has much higher wood density than either *L. tulipifera* or *A. saccharum*, and species with greater wood density tend to have low capacitance (e.g., Meinzer *et al.*, 2008). Unlike *L. tulipifera* and *A. saccharum* that bear large sapwood volume and have low wood density, the small water storage capacity of *Q. alba* cannot provide enough water to limit the rapid drop in water potential due to stomatal water loss, which could also explain its anisohydric behavior (Matheny *et al.* ., 2015) .

More work will be necessary to disentangle the mechanisms contributing to the perplexing hydraulic behavior of *Q. alba* , which are particularly important to understand in light of the long-term and ongoing decline of eastern *Quercus* species (Fei *et al.* ., 2011). *Quercus* decline has been attributed to numerous drivers including fire suppression (Abrams, 2003), climate mesophication (McEwan *et al.* ., 2011), and widespread failure of regeneration and recruitment (Dey, 2014). Given the hydraulic behavior of *Q. alba* observed in our study, water stress may also be an important factor contributing to *Quercus* decline, particularly in the episodic mortality events of mature individuals that are often preceded by drought (Clinton *et al.* ., 1993; Wood *et al.* ., 2018).

### 7.3 Conclusion

To mitigate hydraulic damage, many plant species adhere to a strict coordination between regulation of  $\Psi_L$  and vulnerability to embolism. For common deciduous tree species growing in temperate eastern US forests, we found that the extent of  $\Psi_L$  regulation was not linked to vulnerability of xylem embolism. Specifically, *Q. alba*, an anisohydric species, possessed xylem more vulnerable to embolism than the more isohydric *L. tulipifera* and *A. saccharum* . Moreover, this behavior was generally unaffected by spatio-temporal factors such that coordination among traits were conserved at the species-level. These findings suggest species growing in temperate ecosystems have drought-response traits that are coordinated in a fundamentally different ways than arid climate vegetation. Ultimately, our understanding of plant-water relations may be improved by further investigation into mechanisms which allow plants to tolerate or recover from xylem dysfunction.

### 8. Acknowledgements

We thank D. Tyler Roman, Matthew K. Wenzel, Kathryn O. Shay, Mike P. Voyles, and Daniel C. Ishmael for

assistance with data collection. We acknowledge support from the USDA Forest Service, Southern Research Station, US Department of Energy, through the Terrestrial Ecosystem Science Program and the AmeriFlux Management Project, the National Science Foundation Division of Environmental Biology (grant DEB-1552747 and DEB-1637522) the Integrative Organismal System (IOS-1754893), and the USDA Agriculture and Food Research Initiative (grant 2017-67013-26191 and 2012-67019-19484). JDW acknowledges support for the MOFLUX (US-MOz) site from the U.S. Department of Energy, Office of Science, Office of Biological and Environmental Research Program, through Oak Ridge National Laboratory's Terrestrial Ecosystem Science Focus Area; ORNL is managed by UT-Battelle, LLC, for the U.S. DOE under contract DE-AC05-00OR22725. The authors declare no conflicts of interest.

## 8.1 Author Contributions

MCB and KAN designed the research. MCB, AOC, SOD, JCD, DMJ, JEM, and JDW collected data and performed laboratory analysis. MCB, KAN, and CFM analyzed the data. MCB and KAN wrote the manuscript with input and revisions from all co-authors.

## 9. References

- Abrams, M. D. (2003). Where has all the white oak gone?. *BioScience* **53**, 927-939.
- Addington, R. N., Donovan, L. A., Mitchell, R. J., *et al.* (2006). Adjustments in hydraulic architecture of *Pinus palustris* maintain similar stomatal conductance in xeric and mesic habitats. *Plant, Cell & Environment* **29**, 535-545.
- Ambrose, A. R., Sillett, S. C., & Dawson, T. E. (2009). Effects of tree height on branch hydraulics, leaf structure and gas exchange in California redwoods. *Plant, Cell & Environment* **32**, 743-757.
- Anderegg, W. R. (2015). Spatial and temporal variation in plant hydraulic traits and their relevance for climate change impacts on vegetation. *New Phytologist* **205**, 1008-1014.
- Awad, H., Barigah, T., Badel, E., Cochard, H., & Herbette, S. (2010). Poplar vulnerability to xylem cavitation acclimates to drier soil conditions. *Physiologia Plantarum* **139**, 280-288.
- Bahari, Z. A., Pallardy, S. G., & Parker, W. C. (1985). Photosynthesis, water relations, and drought adaptation in six woody species of oak-hickory forests in central Missouri. *Forest Science* **31**, 557-569.
- Beikircher, B., & Mayr, S. (2009). Intraspecific differences in drought tolerance and acclimation in hydraulics of *Ligustrum vulgare* and *Viburnum lantana*. *Tree Physiology* **29**, 765-775.
- Bond, B. J., & Kavanagh, K. L. (1999). Stomatal behavior of four woody species in relation to leaf-specific hydraulic conductance and threshold water potential. *Tree Physiology* **19**, 503-510.
- Buckley, T. N. (2005). The control of stomata by water balance. *New phytologist* **168**, 275-292.
- Burgess, S. S., Pittermann, J., & Dawson, T. E. (2006). Hydraulic efficiency and safety of branch xylem increases with height in *Sequoia sempervirens* (D. Don) crowns. *Plant, Cell & Environment* **29**, 229-239.
- Charra-Vaskou, K., Charrier, G., Wortemann, R., *et al.* (2012). Drought and frost resistance of trees: a comparison of four species at different sites and altitudes. *Annals of Forest Science* **69**, 325-333.
- Choat, B., Jansen, S., Brodribb, T. J., *et al.* (2012). Global convergence in the vulnerability of forests to drought. *Nature* **491**, 752-755.
- Clinton, B. D., Boring, L. R., & Swank, W. T. (1993). Canopy gap characteristics and drought influences in oak forests of the Coweeta Basin. *Ecology* **74**, 1551-1558.
- Cochard, H., & Tyree, M. T. (1990). Xylem dysfunction in *Quercus*: vessel sizes, tyloses, cavitation and seasonal changes in embolism. *Tree Physiology* **6**, 393-407.

- Cochard, H., Herbette, S., Barigah, T., *et al.* (2010). Does sample length influence the shape of xylem embolism vulnerability curves? A test with the Cavitron spinning technique. *Plant, Cell & Environment* **33**, 1543-1552.
- Dai, A. (2011). Drought under global warming: a review. *Wiley Interdisciplinary Reviews: Climate Change* **2**, 45-65.
- Davis, S. D., Sperry, J. S., & Hacke, U. G. (1999). The relationship between xylem conduit diameter and cavitation caused by freezing. *American journal of botany* **86**, 1367-1372.
- Delzon, S., & Cochard, H. (2014). Recent advances in tree hydraulics highlight the ecological significance of the hydraulic safety margin. *New Phytologist* **203**, 355-358.
- Dey, D. C. (2014). Sustaining oak forests in eastern North America: regeneration and recruitment, the pillars of sustainability. *Forest Science* **60**, 926-942.
- Dietze, M. C., & Moorcroft, P. R. (2011). Tree mortality in the eastern and central United States: patterns and drivers. *Global Change Biology* **17**, 3312-3326.
- Domec, J. C., & Gartner, B. L. (2001). Cavitation and water storage capacity in bole xylem segments of mature and young Douglas-fir trees. *Trees* **15**, 204-214.
- Domec, J. C., & Johnson, D. M. (2012). Does homeostasis or disturbance of homeostasis in minimum leaf water potential explain the isohydric versus anisohydric behavior of *Vitis vinifera* L. cultivars?. *Tree physiology* **32**, 245-248.
- Domec, J. C., Ogée, J., Noormets, A., *et al.* (2012). Interactive effects of nocturnal transpiration and climate change on the root hydraulic redistribution and carbon and water budgets of southern United States pine plantations. *Tree Physiology* **32**, 707-723.
- Durante, M., Maseda, P. H., & Fernandez, R. J. (2011). Xylem efficiency vs. safety: Acclimation to drought of seedling root anatomy for six Patagonian shrub species. *Journal of arid environments* **75**, 397-402.
- Elliott, K. J., & Swank, W. T. (1994). Impacts of drought on tree mortality and growth in a mixed hardwood forest. *Journal of Vegetation Science* **5**, 229-236.
- Fei, S., Kong, N., Steiner, K. C., *et al.* (2011). Change in oak abundance in the eastern United States from 1980 to 2008. *Forest Ecology and Management* **262**, 1370-1377.
- Flory, S. L., & Clay, K. (2010). Non-native grass invasion suppresses forest succession. *Oecologia* **164**, 1029-1038.
- Garcia-Forner, N., Biel, C., Save, R., & Martinez-Vilalta, J. (2017). Isohydric species are not necessarily more carbon limited than anisohydric species during drought. *Tree physiology* **37**, 441-455.
- Gea-Izquierdo, G., Fonti, P., Cherubini, P., *et al.* (2012). Xylem hydraulic adjustment and growth response of *Quercus canariensis* Willd. to climatic variability. *Tree Physiology* **32**, 401-413.
- Gu, L., Pallardy, S. G., Hosman, K. P., & Sun, Y. (2015). Drought-influenced mortality of tree species with different predawn leaf water dynamics in a decade-long study of a central US forest. *Biogeosciences* **12**, 2831-2845.
- Gu, L., Pallardy, S. G., Yang, B., *et al.* (2016). Testing a land model in ecosystem functional space via a comparison of observed and modeled ecosystem flux responses to precipitation regimes and associated stresses in a Central US forest. *Journal of Geophysical Research: Biogeosciences* **121**, 1884-1902.
- Herbette, S., Wortemann, R., Awad, H., *et al.* (2010). Insights into xylem vulnerability to cavitation in *Fagus sylvatica* L.: phenotypic and environmental sources of variability. *Tree physiology* **30**, 1448-1455.

- Hochberg, U., Rockwell, F. E., Holbrook, N. M., & Cochard, H. (2018). Iso/anisohydry: a plant–environment interaction rather than a simple hydraulic trait. *Trends in Plant Science* **23**, 112-120.
- Johnson, D. M., Wortemann, R., McCulloh, K. A., *et al.* (2016). A test of the hydraulic vulnerability segmentation hypothesis in angiosperm and conifer tree species. *Tree physiology* **36**,983-993.
- Kannenber, S. A., & Phillips, R. P. (2020). Non-structural carbohydrate pools not linked to hydraulic strategies or carbon supply in tree saplings during severe drought and subsequent recovery. *Tree Physiology* **40**, 259-271.
- Kennedy, D., Swenson, S., Oleson, K. W., *et al.* (2019). Implementing plant hydraulics in the community land model, version 5. *Journal of Advances in Modeling Earth Systems* **11**,485-513.
- Klein, T. (2014). The variability of stomatal sensitivity to leaf water potential across tree species indicates a continuum between isohydric and anisohydric behaviours. *Functional ecology* **28**,1313-1320.
- Klein, T., Zeppel, M. J., Anderegg, W. R., *et al.* (2018). Xylem embolism refilling and resilience against drought-induced mortality in woody plants: processes and trade-offs. *Ecological research* **33**, 839-855.
- Kocher, P., Horna, V., & Leuschner, C. (2013). Stem water storage in five coexisting temperate broad-leaved tree species: significance, temporal dynamics and dependence on tree functional traits. *Tree physiology* **33**, 817-832.
- Lamy, J. B., Delzon, S., Bouche, P. S., *et al.* (2014). Limited genetic variability and phenotypic plasticity detected for cavitation resistance in a Mediterranean pine. *New Phytologist* **201**,874-886.
- Loewenstein, N. J., & Pallardy, S. G. (1998). Drought tolerance, xylem sap abscisic acid and stomatal conductance during soil drying: a comparison of canopy trees of three temperate deciduous angiosperms. *Tree Physiology* **18**, 431-439.
- Macalady, A. K., & Bugmann, H. (2014). Growth-mortality relationships in pinon pine (*Pinus edulis*) during severe droughts of the past century: shifting processes in space and time. *PloS one* **9**,e92770.
- Maherali, H., & DeLucia, E. H. (2000). Xylem conductivity and vulnerability to cavitation of ponderosa pine growing in contrasting climates. *Tree Physiology* **20**, 859-867.
- Maherali, H., Moura, C. F., Caldeira, M. C., *et al.* (2006). Functional coordination between leaf gas exchange and vulnerability to xylem cavitation in temperate forest trees. *Plant, Cell & Environment* **29**, 571-583.
- Martin-StPaul, N. K., Longepierre, D., Huc, R., *et al.* (2014). How reliable are methods to assess xylem vulnerability to cavitation? The issue of ‘open vessel’ artifact in oaks. *Tree physiology* **34**, 894-905.
- Martinez-Vilalta, J., Cochard, H., Mencuccini, M., *et al.* (2009). Hydraulic adjustment of Scots pine across Europe. *New Phytologist* **184**, 353-364.
- Martinez-Vilalta, J., Poyatos, R., Aguade, D., *et al.* (2014). A new look at water transport regulation in plants. *New phytologist* **204**, 105-115.
- Martinez-Vilalta, J., & Garcia-Forner, N. (2017). Water potential regulation, stomatal behaviour and hydraulic transport under drought: deconstructing the iso/anisohydric concept. *Plant, Cell & Environment* **40**, 962-976.
- Matheny, A. M., Bohrer, G., Garrity, S. R., *et al.* (2015). Observations of stem water storage in trees of opposing hydraulic strategies. *Ecosphere* **6**, 1-13.
- Matheny, A. M., Fiorella, R. P., Bohrer, G., *et al.* (2017). Contrasting strategies of hydraulic control in two codominant temperate tree species. *Ecohydrology* **10**, e1815.

- McDowell, N., Barnard, H., Bond, B., *et al.* (2002). The relationship between tree height and leaf area: sapwood area ratio. *Oecologia* **132**, 12-20.
- McDowell, N., Pockman, W. T., Allen, C. D., *et al.* (2008). Mechanisms of plant survival and mortality during drought: why do some plants survive while others succumb to drought?. *New phytologist* **178**, 719-739.
- McEwan, R. W., Dyer, J. M., & Pederson, N. (2011). Multiple interacting ecosystem drivers: toward an encompassing hypothesis of oak forest dynamics across eastern North America. *Ecography* **34**,244-256.
- Meddens, A. J., Hicke, J. A., Macalady, A. K., *et al.* (2015). Patterns and causes of observed pinon pine mortality in the southwestern United States. *New Phytologist* **206**, 91-97.
- Meier, I. C., & Leuschner, C. (2008). Genotypic variation and phenotypic plasticity in the drought response of fine roots of European beech. *Tree physiology* **28**, 297-309.
- Meinzer, F. C., Campanello, P. I., Domec, J. C., *et al.* (2008). Constraints on physiological function associated with branch architecture and wood density in tropical forest trees. *Tree Physiology* **28**, 1609-1617.
- Meinzer, F. C., & McCulloh, K. A. (2013). Xylem recovery from drought-induced embolism: where is the hydraulic point of no return?. *Tree physiology* **33**, 331-334.
- Meinzer, F. C., Woodruff, D. R., Marias, D. E., *et al.* (2014). Dynamics of leaf water relations components in co-occurring iso-and anisohydric conifer species. *Plant, Cell & Environment* **37**, 2577-2586.
- Meinzer, F. C., Woodruff, D. R., Marias, *et al.* (2016). Mapping ‘hydroscares’ along the iso-to anisohydric continuum of stomatal regulation of plant water status. *Ecology letters* **19**,1343-1352.
- Meinzer, F. C., Smith, D. D., Woodruff, D. R., *et al.* (2017). Stomatal kinetics and photosynthetic gas exchange along a continuum of isohydric to anisohydric regulation of plant water status. *Plant, cell & environment* **40**, 1618-1628.
- Mirfenderesgi, G., Matheny, A. M., & Bohrer, G. (2019). Hydrodynamic trait coordination and cost–benefit trade-offs throughout the isohydric–anisohydric continuum in trees. *Ecohydrology* **12**, e2041.
- Naudts, K., Ryder, J., McGrath, M. J., *et al.* (2015). A vertically discretised canopy description for ORCHIDEE (SVN r2290) and the modifications to the energy, water and carbon fluxes. *Geoscientific Model Development* **8**, 2035-2065.
- Novick, K., Oren, R., Stoy, P., *et al.* (2009). The relationship between reference canopy conductance and simplified hydraulic architecture. *Advances in Water Resources* **32**, 809-819.
- Novick, K. A., Ficklin, D. L., Stoy, P. C., *et al.* (2016). The increasing importance of atmospheric demand for ecosystem water and carbon fluxes. *Nature climate change* **6**, 1023-1027.
- Novick, K. A., Konings, A. G., & Gentine, P. (2019). Beyond soil water potential: An expanded view on isohydricity including land–atmosphere interactions and phenology. *Plant, cell & environment* **42**, 1802-1815.
- Ogasa, M., Miki, N. H., Murakami, Y., & Yoshikawa, K. (2013). Recovery performance in xylem hydraulic conductivity is correlated with cavitation resistance for temperate deciduous tree species. *Tree physiology* **33**, 335-344.
- Oishi, A. C., Oren, R., Novick, K. A., *et al.* (2010). Interannual invariability of forest evapotranspiration and its consequence to water flow downstream. *Ecosystems* **13**, 421-436.
- Oishi, A. C., Miniati, C. F., Novick, K. A., *et al.* (2018). Warmer temperatures reduce net carbon uptake, but do not affect water use, in a mature southern Appalachian forest. *Agricultural and forest meteorology* **252**, 269-282.

- Olivier, M. D., Robert, S., & Fournier, R. A. (2016). Response of sugar maple (*Acer saccharum*, Marsh.) tree crown structure to competition in pure versus mixed stands. *Forest Ecology and Management* **374**, 20-32.
- Pan, Y., Chen, J. M., Birdsey, R., *et al.* (2011). Age structure and disturbance legacy of North American forests. *Biogeosciences* **8**, 715-732.
- Phillips, N., Oren, R., & Zimmermann, R. (1996). Radial patterns of xylem sap flow in non-, diffuse-and ring-porous tree species. *Plant, Cell & Environment* **19**, 983-990.
- Plaut, J. A., Yezpez, E. A., Hill, J., *et al.* (2012). Hydraulic limits preceding mortality in a pinon-juniper woodland under experimental drought. *Plant, Cell & Environment* **35**, 1601-1617.
- Roman, D. T., Novick, K. A., Brzostek, E. R., *et al.* (2015). The role of isohydric and anisohydric species in determining ecosystem-scale response to severe drought. *Oecologia* **179**, 641-654.
- Scholz, F. G., Phillips, N. G., Bucci, S. J., *et al.* (2011). Hydraulic capacitance: biophysics and functional significance of internal water sources in relation to tree size. In *Size-and age-related changes in tree structure and function* (pp. 341-361). Springer, Dordrecht.
- Scholz, A., Klepsch, M., Karimi, Z., & Jansen, S. (2013). How to quantify conduits in wood?. *Frontiers in plant science* **4**, 56.
- Schweingruber, F. H. (2007). Preparation of wood and herb samples for microscopic analysis. *Wood Structure and Environment* , 3-5. Springer, Berlin, Heidelberg.
- Schultz, H. R. (2003). Differences in hydraulic architecture account for near-isohydric and anisohydric behaviour of two field-grown *Vitis vinifera* L. cultivars during drought. *Plant, Cell & Environment* **26**, 1393-1405.
- Skelton, R. P., West, A. G., & Dawson, T. E. (2015). Predicting plant vulnerability to drought in biodiverse regions using functional traits. *Proceedings of the National Academy of Sciences* **112**, 5744-5749.
- Skelton, R. P., Dawson, T. E., Thompson, S. E., *et al.* (2018). Low vulnerability to xylem embolism in leaves and stems of North American oaks. *Plant Physiology* **177**, 1066-1077.
- Sperry, J. S., & Saliendra, N. Z. (1994). Intra-and inter-plant variation in xylem cavitation in *Betula occidentalis*. *Plant, Cell & Environment* **17**, 1233-1241.
- Sperry, J. S., Hacke, U. G., Oren, R., & Comstock, J. P. (2002). Water deficits and hydraulic limits to leaf water supply. *Plant, cell & environment* **25**, 251-263.
- Sperry, J. S., & Love, D. M. (2015). What plant hydraulics can tell us about responses to climate-change droughts. *New Phytologist* **207**, 14-27.
- Swank, W. T., & Webster, J. R. (Eds.). (2014). *Long-term response of a forest watershed ecosystem: Clearcutting in the southern Appalachians* . Oxford University Press, New York.
- Taneda, H., & Sperry, J. S. (2008). A case-study of water transport in co-occurring ring-versus diffuse-porous trees: contrasts in water-status, conducting capacity, cavitation and vessel refilling. *Tree physiology* **28**, 1641-1651.
- Tardieu, F., & Simonneau, T. (1998). Variability among species of stomatal control under fluctuating soil water status and evaporative demand: modelling isohydric and anisohydric behaviours. *Journal of experimental botany* **49**, 419-432.
- Thomsen, J. E., Bohrer, G., Matheny, A. M., *et al.* (2013). Contrasting hydraulic strategies during dry soil conditions in *Quercus rubra* and *Acer rubrum* in a sandy site in Michigan. *Forests* **4**, 1106-1120.
- Torres-Ruiz, J. M., Cochard, H., Mayr, S., *et al.* (2014). Vulnerability to cavitation in *Olea europaea* current-year shoots: further evidence of an open-vessel artifact associated with centrifuge and air-injection

techniques. *Physiologia Plantarum* **152**,465-474.

Trifilo, P., Kiorapostolou, N., Petruzzellis, F., *et al.* (2019). Hydraulic recovery from xylem embolism in excised branches of twelve woody species: Relationships with parenchyma cells and non-structural carbohydrates. *Plant Physiology and Biochemistry* **139**,513-520.

Trabucco, A., & Zomer, R. J. (2009). Global aridity index (global-aridity) and global potential evapotranspiration (global-PET) geospatial database. *CGIAR Consortium for Spatial Information* .

Turner, N. C. (1988). Measurement of plant water status by the pressure chamber technique. *Irrigation science* **9**, 289-308.

Tyree, M. T., & Sperry, J. S. (1989). Vulnerability of xylem to cavitation and embolism. *Annual review of plant biology* **40**, 19-36.

Tyree, M. T., & Zimmermann, M. H. (2013). *Xylem structure and the ascent of sap* . Springer, Berlin, Germany

Vose, J. M., & Elliott, K. J. (2016). Oak, fire, and global change in the eastern USA: What might the future hold?. *Fire Ecology* **12**, 160-179.

Wolfe, B. T., Sperry, J. S., & Kursar, T. A. (2016). Does leaf shedding protect stems from cavitation during seasonal droughts? A test of the hydraulic fuse hypothesis. *New Phytologist* **212**,1007-1018.

Wood, J. D., Knapp, B. O., Muzika, R. M., *et al.* (2018). The importance of drought–pathogen interactions in driving oak mortality events in the Ozark Border Region. *Environmental Research Letters* **13**, 015004.

Wortemann, R., Herbette, S., Barigah, T. S., *et al.* (2011). Genotypic variability and phenotypic plasticity of cavitation resistance in *Fagus sylvatica* L. across Europe. *Tree physiology* **31**,1175-1182.

Yi, K., Dragoni, D., Phillips, R. P., Roman, D. T., & Novick, K. A. (2017). Dynamics of stem water uptake among isohydric and anisohydric species experiencing a severe drought. *Tree physiology* **37**, 1379-1392.

Zeppel, M. J., Anderegg, W. R., Adams, H. D., *et al.* (2019). Embolism recovery strategies and nocturnal water loss across species influenced by biogeographic origin. *Ecology and evolution* **9**, 5348-5361.

## 10. Tables

**Table 1.** Climate and sampled tree species across the ten forest sites.

Region	Stand	Species Sampled	Canopy Height (m)	Soil Type	Aridity Index	Me
NC_W	15yo	<i>L. tulipifera</i> , <i>Q. alba</i>	4.5	Fine-Loamy	1.478	180
	35yo	<i>L. tulipifera</i> , <i>Q. alba</i>	17			
	85yo	<i>L. tulipifera</i> , <i>Q. alba</i>	35			
IN	15yo	<i>L. tulipifera</i> , <i>Q. alba</i>	5	Silt Clay Loam	0.928	103
	35yo	<i>L. tulipifera</i> , <i>Q. alba</i>	20			
	85yo	<i>A. saccharum</i> , <i>L. tulipifera</i> , <i>Q. alba</i>	30			
NC_E	15yo	<i>A. saccharum</i>	9.2	Gravelly-Loam	0.811	114
	35yo	<i>A. saccharum</i> , <i>L. tulipifera</i> , <i>Q. alba</i>	15.1			
	85yo	<i>L. tulipifera</i> , <i>Q. alba</i>	27.5			
MO	85yo	<i>A. saccharum</i> , <i>Q. alba</i>	18.5	Silt-Loam	0.744	986

**Table 2.** Summary statistics of test between subjects for vulnerability thresholds from two-way ANOVA with species and age as fixed factors and region as a blocking factor.

	Dependent Variable	df	Mean Square	F	p
<b>Species</b>	P12	2	17.033	<b>149.87</b>	<b>0.001</b>
<b>Age</b>	P12	2	0.46	0.40	0.702
<b>Region</b>	P12	3	0.444	0.37	0.784
<b>Species*Age</b>	P12	2	0.018	0.07	0.935
<b>Species*Region</b>	P12	3	0.113	0.05	0.727
<b>Age*Region</b>	P12	3	1.229	4.81	0.115
<b>Species*Age*Region</b>	P12	3	0.255	0.61	0.611
<b>Species</b>	P50	2	33.719	<b>169.62</b>	<b>0.003</b>
<b>Age</b>	P50	2	0.545	0.49	0.656
<b>Region</b>	P50	3	0.556	0.37	0.78
<b>Species*Age</b>	P50	2	0.058	<b>18.88</b>	<b>0.017</b>
<b>Age*Region</b>	P50	3	1.21	<b>21.31</b>	<b>0.016</b>
<b>Species*Age*Region</b>	P50	3	0.057	0.10	0.959

**Table 3.** Summary statistics of test between subjects for xylem anatomy from two-way ANOVA with species and age as fixed factors.

	Dependent Variable	df	Mean Square	F	p
<b>Species</b>	Vessel Lumen Area	1	1854153	<b>169.95</b>	<b>&lt;0.001</b>
<b>Age</b>	Vessel Lumen Area	2	2776	0.25	0.776
<b>Species*Age</b>	Vessel Lumen Area	2	10909	0.04	0.958
<b>Species</b>	Vessel Density	1	9617763	<b>270.64</b>	<b>&lt;0.001</b>
<b>Age</b>	Vessel Density	2	27053	0.76	0.471
<b>Species*Age</b>	Vessel Density	2	35537	2.09	0.133

## 11. Figure Legends

*Figure 1: Stand regions and moisture conditions across eastern United States deciduous forests. Aridity index values are mean Aridity-Witness Index (calculated as the fraction of mean annual precipitation to mean annual evapotranspiration) at 9 m spatial resolution from 1970–2000. Aridity index data were accessed from the CGIAR-CSI GeoPortal at <https://cgiarcsi.community> (Trabucco & Zomer, 2009).*

*Figure 2: Assessing the bias from open-vessel artifacts. Panel (a) and (d) are individual *Q. alba* and *L. tulipifera* embolism curves generated from samples collected in NC 85yo, Panel (b) (c) and (e) (f) are a comparison of threshold means across all samples from a one-way ANOVA between *Q. alba* and *L. tulipifera* respectively when partitioned by ‘r’ and ‘s’ shaped curves. Error bars are  $\pm 1$  standard error of the mean. Βαρς νοτ σηαρινγ τηε σαμε λεττερς δενοτε σιγνιφιζαντ διφφερενζεσ ατ  $\alpha = 0.05$*

*Figure 3: Embolism thresholds across forest stands. Panel (a) and (b) are mean P12 and P50 values ( $\pm SE$ ), respectively. Numbers above bars are sample size. Groups of bars not sharing the same uppercase letters denote significant differences among species determined by a two-way ANOVA with species and age as fixed factors and region as a blocking factor (Table 2).*

*Figure 4: Test of simple effects of significant interaction terms from two-way ANOVA by pairwise comparison of least square means. Panel (a) is least square mean P50 ( $\pm SE$ ) across forest ages for each species. Panel (b) is least square mean P50 ( $\pm SE$ ) αρσοσ ζηρονοσεχευενζε ρεγιοιζ φορ εαση φορεστ αγε. Γρουπς οφ βαρς*

νοτ σηαρινγ τη σαμε υππερσασε λεττερς δενοτε σηγνιφισαντ διφφερενςες οφ μαιν εφφερςτς ατ  $a = 0.05$ . Ωιτην γρουπς, βαρς νοτ σηαρινγ τη σαμε λωερσασε λεττερς δενοτε σηγνιφισαντ διφφερενςες ατ  $a = 0.05$ .

Figure 5. Mean xylem lumen area ( $\pm SE$ ) of *Q. alba* and *L. tulipifera* samples across chronosequences (Panel (a)) and age (Panel (c)). Groups of bars not sharing the same uppercase letters denote significant differences ( $p [?] 0.05$ ) between species, while bars within groups not sharing letters denote differences within species among ages or chronosequences from a two-way ANOVA with species and age as fixed factors. Panels (b) and (d) show the relationship between mean lumen area and mean specific embolism threshold of individual trees assessed by linear regression. Lines are best fit from linear regression when slope is significant ( $p [?] 0.05$ ).

Figure 6: Mean vessel density ( $\pm SE$ ) of *Q. alba* and *L. tulipifera* and samples across chronosequences (Panel (a)) and age (Panel (c)). Groups of bars not sharing the same uppercase letters denote significant differences ( $p [?] 0.05$ ) between species, while bars within groups not sharing letters denote differences within species among ages or chronosequences from a two-way ANOVA with species and age as fixed factors and region as a blocking factor (Table 2). Panel (b) and (d) show the relationship between mean lumen area and mean specific embolism threshold of individual trees assessed by linear regression. Lines are best fit from linear regression when slope is significant ( $p [?] 0.05$ ). Solid lines are best fit across species and dashed line is at the species-level.

Φηγυρε 7: Μιδδαψ λεαφ ωατερ ποτεντιαλ ( $\Psi_{\Delta}$ ) οβσερατιονς αςροος σπεςιες ανδ στανδς. Πανελ (α) ις  $\Psi_{\Delta}$  ιντερχυαρτιλε ρανγε ιν εαση ρεσπεςτιε στανδ. Βοξ-πλοτς σηωω τη μεδιαν (μιδδλε λινε), ιντερχυαρτιλε ρανγε (βοξ), ανδ μαξιμυμ/μινιμυμ αλυε (ωηιοκερς), εξςεπτ ωηερε αλυες εξςεεδ 1.5 τιμες τη ιντερχυαρτιλε ρανγε (ποιντς). Νυμβερς αβοε βοξες αρε σαμπλε σιζε. Πανελ (β) ις μεαν ιντερχυαρτιλε ρανγε ( $\pm SE$ ) φορ εαση σπεςιες. Βαρς νοτ σηαρινγ τη σαμε υππερσασε λεττερς δενοτε σηγνιφισαντ διφφερενςες αςροος σπεςιες βψ α τωο-ωαψ ANOVA ωιτη σπεςιες ανδ αγε ας φιξεδ φαςτορς.

Φηγυρε 8: Διφφερενςες βετωεεν ισοηψδρις βεηαιορ ανδ εμβολισμ τηρεσηολδς. Ισοηψδρις σπεςιες αρε *L. τυλιπιφερα* ανδ *A. σαςσηαρυμ*. Αιςοηψδρις σπεςιες αρε *X. αλβα*. Πανελ (α) ανδ (ς) αρε μεαν Π12 ανδ Π50 αλυες ( $\pm SE$ ), ρεσπεςτιελψ. Βαρς νοτ σηαρινγ τη σαμε υππερσασε λεττερς δενοτε σηγνιφισαντ διφφερενςες (π [:] 0.05) φορμ τωο-ταιλεδ τ-τεστ.

Φηγυρε 9: Ρελατιονσηιπ βετωεεν  $\Psi_{\sigma\alpha\phi\epsilon\tau\psi}$  ανδ  $\Psi_{\Delta}$  ιντερχυαρτιλε ρανγε. Πανελ (α) ις σαφετψ μαργιν ατ Π12 ανδ Πανελ (β) ις σαφετψ μαργιν ατ Π50. Σολιδ λινες αρε βεστ φιτ λινεαρ ρεγρεσσιον αςροος σπεςιες ωηεν ολοπε ις σηγνιφισαντ (π [:] 0.05).

## 12. Φηγυρες

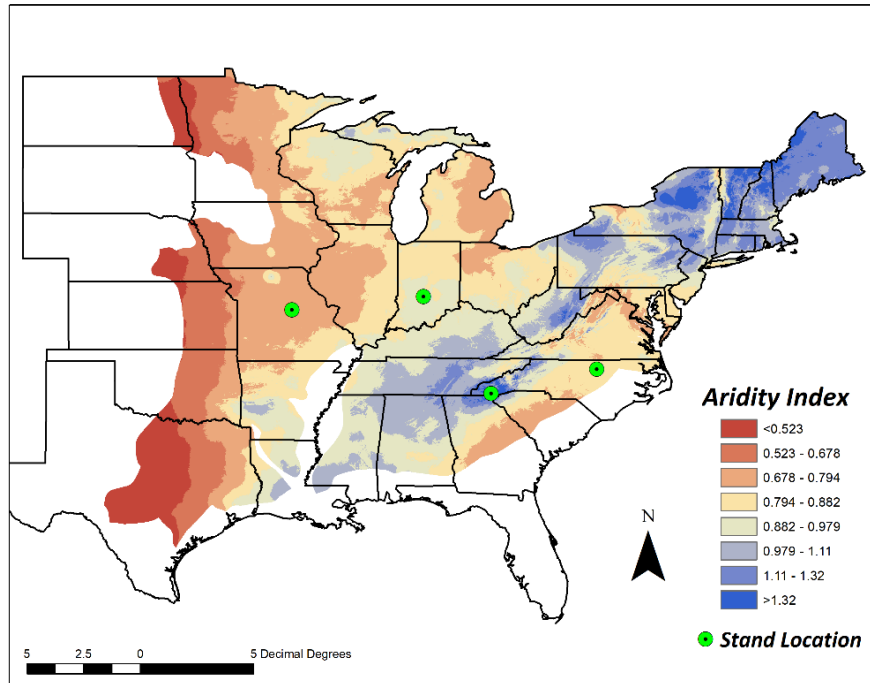


**Figure 1.** Stand regions and moisture conditions across eastern United States deciduous forests. Aridity index values are mean Aridity-Witness Index (calculated as the fraction of mean annual precipitation to mean annual evapotranspiration) at 9 m spatial resolution from 1970–2000. Aridity index data were accessed from the CGIAR-CSI GeoPortal at <https://cgiarcsi.community> (Trabucco & Zomer, 2009).

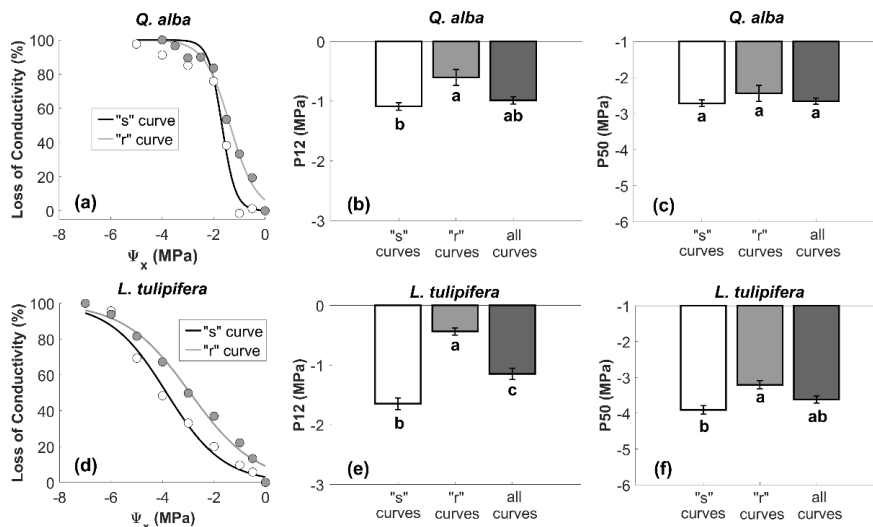


**Figure 2.** Assessing the bias from open-vessel artifacts. Panel (a) and (d) are individual *Q. alba* and *L. tulipifera* embolism curves generated from samples collected in NC 85yo, Panel (b) (c) and (e) (f) are a comparison of threshold means across all samples from a one-way ANOVA between *Q. alba* and *L. tulipifera* respectively when partitioned by 'r' and 's' shaped curves. Error bars are  $\pm 1$  standard error of the mean. Bars not sharing the same letters denote significant differences at  $\alpha = 0.05$ .

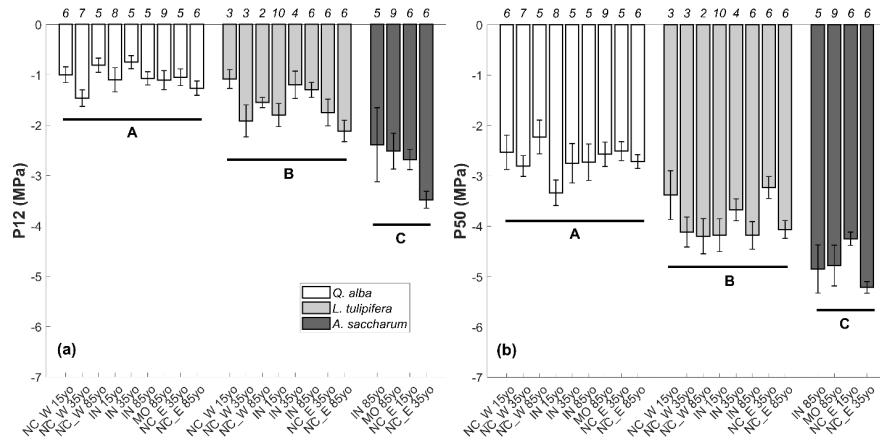


**Figure 3.** Embolism thresholds across forest stands. Panel (a) and (b) are mean P12 and P50 values ( $\pm$ SE), respectively. Numbers above bars are sample size. Groups of bars not sharing the same uppercase letters denote significant differences among species determined by a two-way ANOVA with species and age as fixed factors and region as a blocking factor (Table 2).

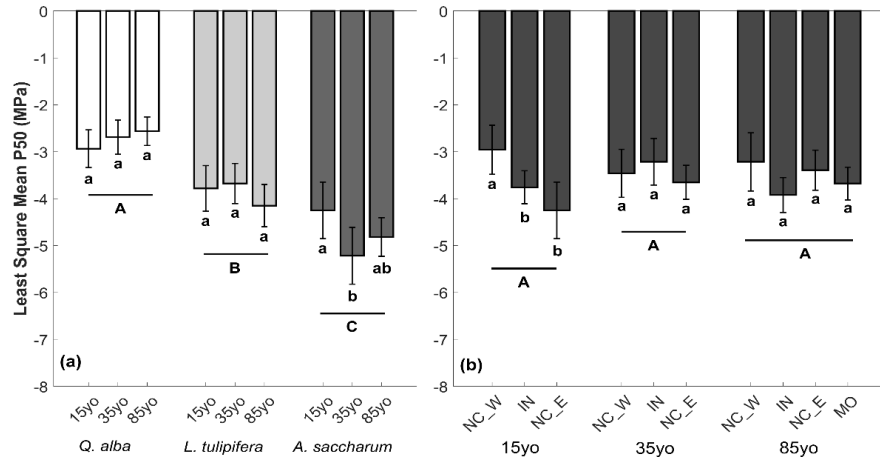


**Figure 4.** Test of simple effects of significant interaction terms from two-way ANOVA by pairwise comparison of least square means. Panel (a) is least square mean P50 ( $\pm$ SE) across forest ages for each species. Panel (b) is least square mean P50 ( $\pm$ SE) across chronosequence regions for each forest age. Groups of bars not sharing the same uppercase letters denote significant differences of main effects at  $\alpha = 0.05$ . Within groups, bars not sharing the same lowercase letters denote significant differences at  $\alpha = 0.05$ .

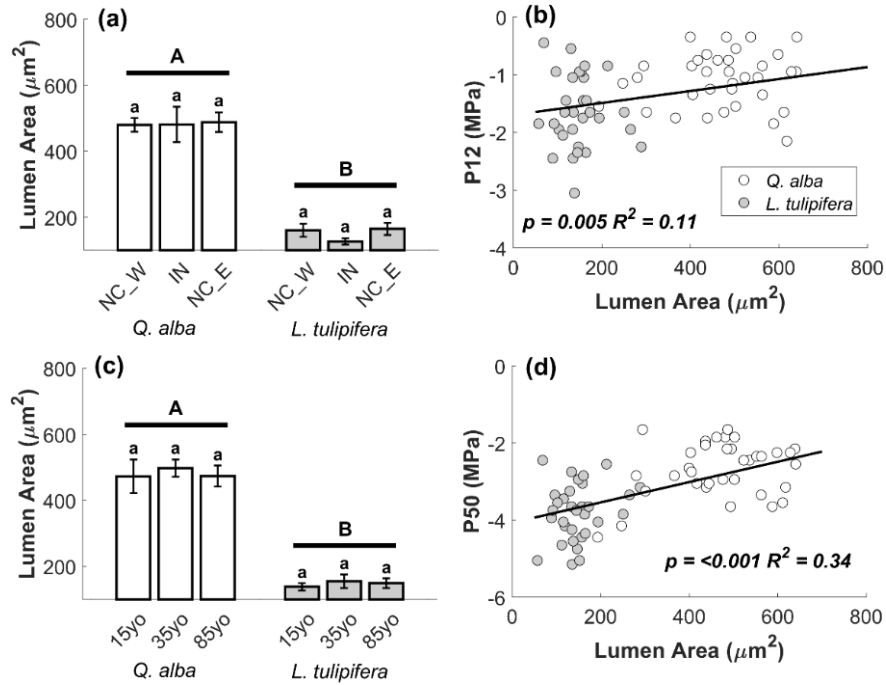


**Figure 5.** Mean xylem lumen area ( $\pm$ SE) of *Q. alba* and *L. tulipifera* samples across chronosequences (Panel (a)) and age (Panel (c)). Groups of bars not sharing the same uppercase letters denote significant differences ( $p \leq 0.05$ ) between species, while bars within groups not sharing letters denote differences within species among ages or chronosequences from a two-way ANOVA with species and age as fixed factors. Panels (b) and (d) show the relationship between mean lumen area and mean specific embolism threshold of individual trees assessed by linear regression. Lines are best fit from linear regression when slope is significant ( $p \leq 0.05$ ).

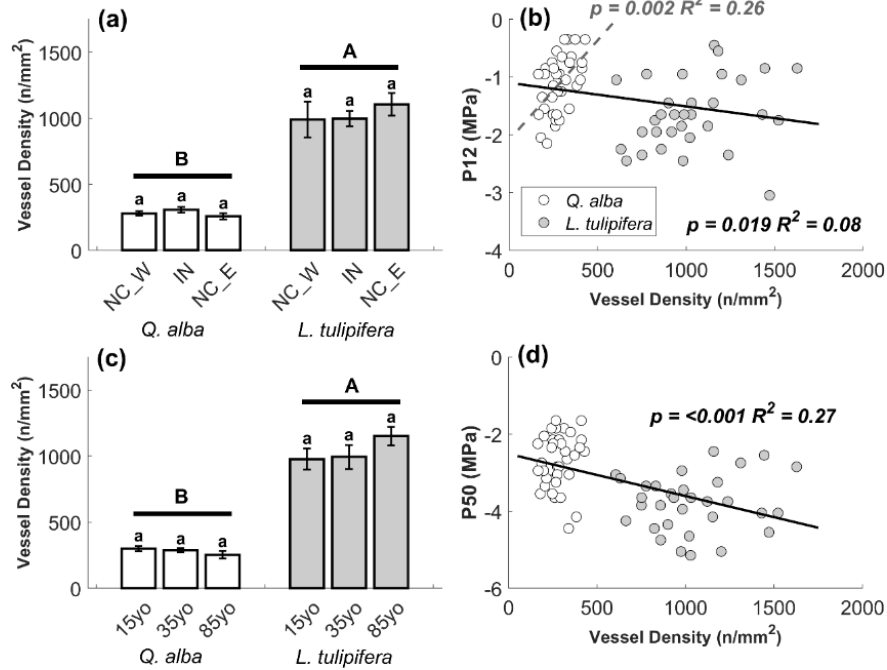


**Figure 6.** Mean vessel density ( $\pm$ SE) of *Q. alba* and *L. tulipifera* and samples across chronosequences (Panel (a)) and age (Panel (c)). Groups of bars not sharing the same uppercase letters denote significant differences ( $p \leq 0.05$ ) between species, while bars within groups not sharing letters denote differences within species among ages or chronosequences from a two-way ANOVA with species and age as fixed factors and region as a blocking factor (Table 2). Panel (b) and (d) show the relationship between mean lumen area and mean radius specific embolism threshold of individual trees assessed by linear regression. Lines are best fit from linear regression when slope is significant ( $p \leq 0.05$ ). Solid lines are best fit across species and dashed line is at the species-level.

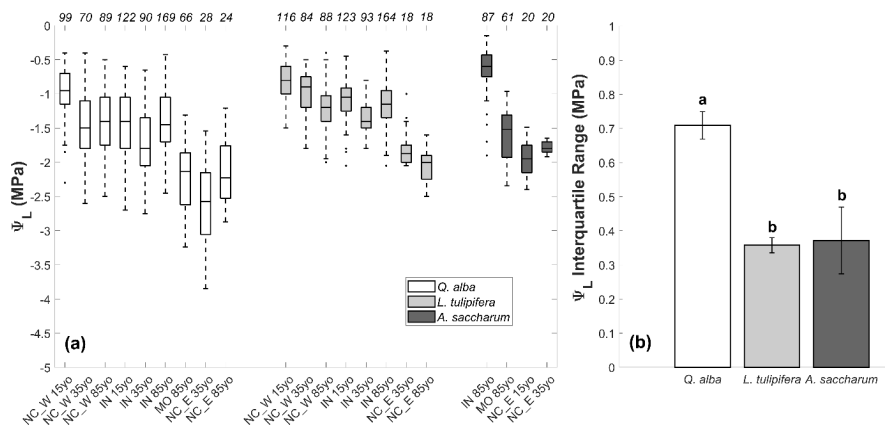


**Figure 7.** Midday leaf water potential ( $\Psi_L$ ) observations across species and stands. Panel (a) is  $\Psi_L$  interquartile range in each respective stand. Box-plots show the median (middle line), interquartile range (box), and maximum/minimum value (whiskers), except where values exceed 1.5 times the interquartile range (points). Numbers above boxes are sample size. Panel (b) is mean interquartile range ( $\pm$ SE) for each species. Bars not sharing the same uppercase letters denote significant differences across species by a

two-way ANOVA with species and age as fixed factors.

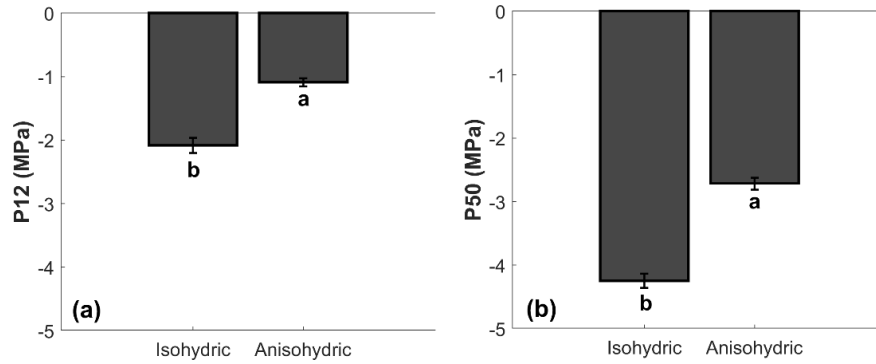


**Figure 8.** Differences between isohydric behavior and embolism thresholds. Isohydric species are *L. tulipifera* and *A. saccharum*. Anisohydric species are *Q. alba*. Panel (a) and (c) are mean P12 and P50 values ( $\pm$ SE), respectively. Bars not sharing the same uppercase letters denote significant differences ( $p < 0.05$ ) from two-tailed  $t$ -test.

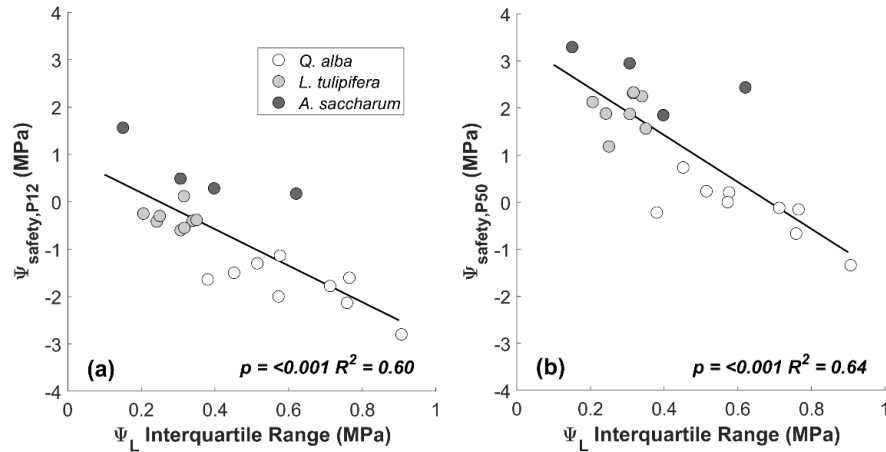


**Figure 9.** Relationship between  $\Psi_{\text{safety}}$  and  $\Psi_L$  interquartile range. Panel (a) is safety margin at P12 and Panel (b) is safety margin at P50. Solid lines are best fit linear regression across species when slope is significant ( $p < 0.05$ ).